Chapter

Landslide Analysis over Creep Theory - Crack Propagation of Shale Slopes in Şırnak Asphaltite Coal Mine Site 1 and 2

Yildirim İsmail Tosun

Abstract

The soft rock and wet slopes increase landslides over 50 m long creep slide and risk assessment for long steep slide in Şırnak open-pit coal mining should be searched in asphaltite quarries. The Avgamasya quarries No1 and 2 at critical depths and road bench sites in Şırnak, reaching over 120 m height with 60–65° shale slopes, developing major creep factors and other factors for landslide in the deep quarry locations is resulting debris rock falling or free sliding. The pore pressure measurements by measurements of water levels in four wells and water flow counting as the mining safety in recent years. This research provided rock slope stability patterns and crack propagation control of the hazardous location and formation cracks. The stages of creep experimentation explored the geophysical characteristics and thaw and freeze testing of rock samples. For this aim, two different long sliding areas with similar geoseismical conditions, two main analyzing methods, and patterns of researches were developed. Firstly, data on crack propagation *in situ* rock shale faces over certain time periods were determined. Displacement measurements over highly saturated shale—limestone contacts over the base of crack counting in a meter scale such as Rock Quality Designation (RQD) scoring of drilling logs. Secondly, hydrological water level logs were taken into consideration. On the other hand, due to that creep effect over freeze crack propagation unseen cause instability over wet sliding surfaces over 50 m, long sliding surface matter over slopes, poly linear or circle type creep sliding or rock tumbling falling failure types, and GEO5 slope stability, slice analysis will be advantageous instead of Finite Element Method (FEM) method.

Keywords: landslide analysis, Şırnak asphaltite quarry, active potential landslide, creep failure, geotechnical stability, GEO5 slope stability

1. Introduction

The time-dependent failure propagation occurs on the local mountainous natural rockfalls in the hard winter conditions of freezing and thaw cycles observed on road slopes. Hazardous deep quarries in the Şırnak will make a great concern in asphaltite production as significant to the local economy. The hydrology of the area,

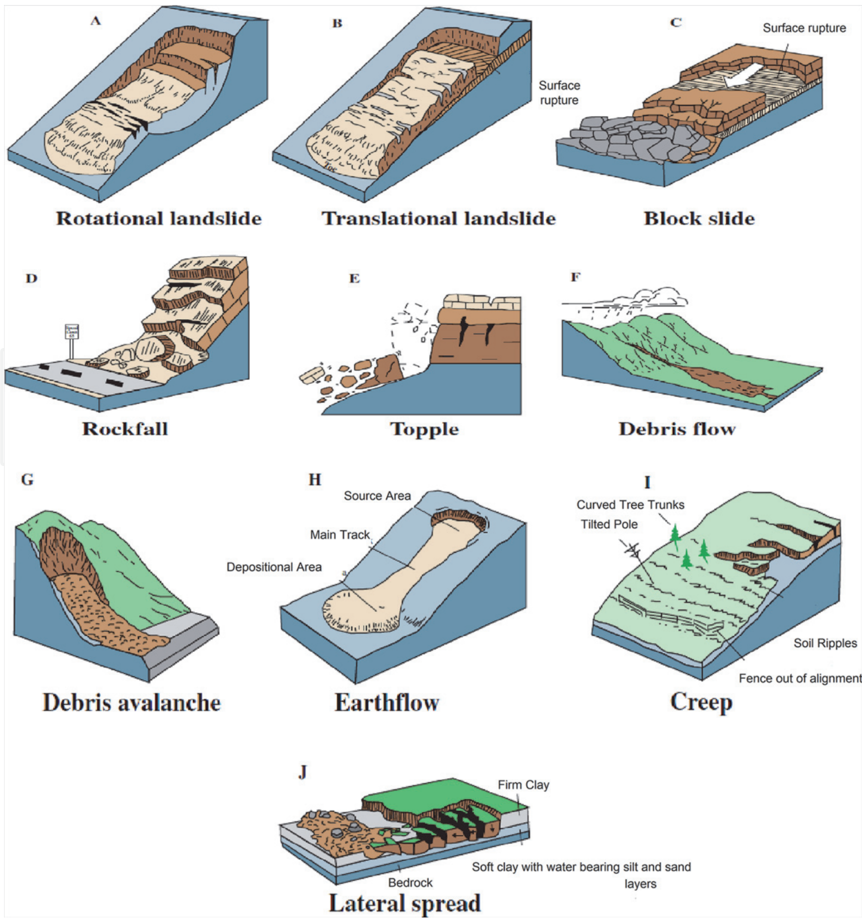

Quarry medium/ soft rock Failure cause: water content
Quarry medium/ soft rock, road slope, mountain steep hill Failure cause: water content and creep
Quarry medium/ soft rock, road slope, medium hill, urbanization area Failure cause: flood, water content, creep

Table 1.
Creep effect and type of landslides, the sites observed [1].

few months hard fill snow on the quarry avoiding production is important in creep failure or landslides as illustrated in **Table 1** [1] due to loosen rock fallings and free slide of saturated shale slopes over safety limit grade zone [1–3]. Formations such as shale in the regional quarries allow crack propagation by freeze and thaw cycling in the winter climates [4, 5]. The pore structure and low mechanical strength cause a negative effect on creep-dependent breakage quality and stone falling [6–9]. For this reason, the freeze-thaw cycling time and crack texture were critical for creep behavior at the local slope durability [10–12].

Although the 65° (72°gr) of bench slopes of quarries 1 and 2 as steeper will reduce the excavation costs, it has a negative effect on the creep stability of the quarry at the end of winter, opening the excavation over melted ice period. The highly fractured rock masses have undergone crack propagation, extremely fractured, and showed counting effects on RQD values. The geological strength index GIS, Rock Mass Rating (RMR), and RQD points were determined, by creep texture properties of rock mass in the classification ensured long-term planning stability in the coal quarry excavations [11].

It is quite difficult to creep the block samples depending on the quarry development. Various rock mass classification methods have been proposed. The high groundwater levels and water pressure make ease landslides in the quarry caused major problems in terms of safety. The creep effect in rock mass assessment by freeze and thaw test method is proposed. Q classification system and the Hoek–Brown empirical failure criterion [6–8] were most frequently used by researchers. By the high creep matter, the geomechanical properties critically change the sawing rate resulting in failure by lowering the shear strength and similar methods are used.

The creep failure in rock masses is dependent on discontinuity features that controlled crack face filling and roughness. The slopes failures and discontinuity-controlled failures can be divided into creep discontinuity failures that critically occur in heterogeneous rock conditions as alluvial shale mixed formations. Those creep failures cannot be controlled. The failures are severely fractured and cracked and time depended propagated unseen. It mainly occurs in highly weathered rock masses [6–10].

In the stability analysis, the shear strength of the rock mass at the time of failure was determined. The water pressure parameters for all sliding geometry of the failure surface should be analyzed by the calculated block weight slice method. This method is used in soft rock and heterogeneous rock masses although it describes the failures that occur [1–5], the rock masses are also linear or irregular failure envelopes in different soft rock mass and heterogeneity. However, this cannot fully calculate by the medium the shear strength.

Therefore, The Mohr–Coulomb method is not a preferred measure of instability for rock mass in creep propagation. In the failures that occur in soft and heterogeneous rock masses, Hoek–Brown [6–8] failure criterion is more preferred for the determination of geomechanical strength change.

On quarries no 1 and 2, the south side shale and altered alluvial debris covers and groundwater levels increase in September and reach the highest level in April. December-February period of mining is a closed and active time for creep crack propagation even saturation time [11–14]. The water level increase and freeze and thaw cycle causes of the rock failures occur determined by extensive *in situ* tests. Planning attention to slope geometry in the quarry asphaltite facings contact to water level, drainage, and overburden excavation operations can start in March at the highest water flow of April reaching 50+% filling the bottom of the pit. In order to understand the creep mechanism of slopes S1, S2, S3, and S4 is the main essential issues. While the study is designing the critical hazardous slopes, the geotechnical properties of the rock mass receiving data from the Los Angeles and Blade Sawing tests, freeze-thaw Unaxial Compresssive Strength (UCS) strength is determined [15–20]. Slope angles should be planned considering the quarry safety with a factor count of 1, 35 by GEO5 Slope Stability software. The creep determination process is carried out by freeze-thaw analysis [6].

1.1 Geology in asphaltite quarry in Avgamasya, Şırnak

Study area geology sedimentary alluvial, shale, and calcareous rocks of the Gercus Massif formation Jurassic aged in the Avgamasya, Şırnak province. There are highly disseminated chlorites and calcites are exposed (**Figure 1**). In the southern part, the late Mesozoic aged limestone anticline zone, in the northern part early Eosin age altered porous limestone calcite are located heterogeneous shale contact to Cudi formation and Cizre formation.

In the field studies, the study including the open-pit area has a very heterogeneous layered shale and alluvial contact with vertical asphaltite structure. (**Figure 1**). The hazardous areas of asphaltite quarries are studied as slopes S1, S2, S3, and S4 over the excavation area. The discontinuity intervals were determined. The creep act by freeze and thaw effect is critical for time-dependent rock loose and free landslides developing in mining quarries and urbanization lands in the Southeastern Anatolian regions at height over 1400 m attitudes by high tectonically soft ground conditions [10–14]. The instability of rock loss in the asphaltite coal quarry area creep cracks were developed with advanced mining operations over decades and loosen geotechnical characters of soft heterogeneous formations determined. The detailed investigations in the quarries during mining operations have two fundamental causes of free sliding over freeze and thaw effect on the geotechnical conditions [15–21]. First

(a)

(b)

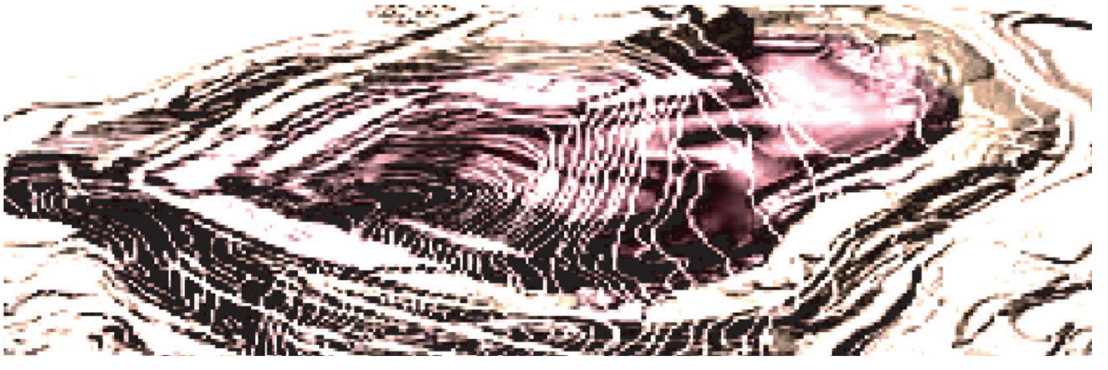

Figure 1.
(a and b) View and contour topography of Avgamasya No 1 pit Şırnak asphaltite coal mine site and survey area 1/5000.

of all, the tumbling rock falling landslides occurred at the top of the quarries by groundwater saturation and hard rainwater taking surface conditions as clearly seen. In terms of the past, fatal disasters of instability were observed widely in the different quarries. Secondly, free flow sliding land rocks as debris flows as land flows were similar to the other high deep quarries [22–34]. Therefore, stability conditions and soft rock properties causing past landslides and rock tumbling were so important in order to evaluate and criticize that may develop in the mining excavation areas and even urbanization areas [34–44]. Debris areas or possible free flow loosen landfill areas in mountainous and high-steep rocks were evaluated for free creep flow and tumbling depending on the topology. The unsuitable land use for urbanization over hills increases the creep probability for the development of free land flows [45–53]. In the case of creep landslides, the stability analysis revised by time and related to crack propagation can be achieved and change the safety factor on avoiding the fatal disasters of the quarry or urbanization area concerned [54–60].

The stability analyzes of the top benches in quarries 1 and 2 south side slopes are managed to protect the asphaltite coal excavation equipment and fatal casualties caused by landslides. For this aim, in the quarries 1 and 2 slopes S1, S2, S3, and S4, the free slide top benches three over 35 m long sliding surface excavation area are considered. The fatal experiences of Şırnak Avgamasya and Silopi open-pit mining were carrying high landslide or rock falling risk (**Figure 1**) [11–14]. The creep effect over soft mechanical properties of the soft rock formations of soft limestone, alluvium, and shale layers heterogeneously oriented in the vertical belt form where creep rock falling or free top land flows occurred in the asphaltite quarries. The poly linear surface or circle shape slope stability analyzes for top benches are carried out with GEO5 Slope stability software and GEO5 FEM methods. The slice weight charts of the GEO5 program on the scope of this investigation regarding creep effect, a 1/5000 scale quarry no 1 bench isocontour map covering 3.7 km^2 of the study area are shown in **Figure 1a** and **b**. The high risk of tumbling top rocks and free flow uncohesive sliding over the asphaltite excavation zone is seen as shown in **Figure 2a** and **b**. The blackish zone area is representing a wet asphaltite coal extraction area.

The asphaltite excavation is carried out over 2–4 m thick asphaltite seam placed vertical whirled form in the limestone rock with approximately somehow 1/2 m thick at 62° to SE and approximately 10–25 m for shale 87° to NW and completely changed the orientation to horizontal layer (**Figures 2-4**). The discontinuity surfaces were slightly flat in limestone. It is clear that the crack surfaces are quite slippery in shale rocks. The shale rock mass in the Şırnak quarry pit is extremely fractured (**Figures 3** and **4**). Since it is fractured and heavily weathered over alluvial heterogeneous layers mainly controls free sliding by water saturation and expected collection at the contact surface. In this type of rock formation, landslides and creep failures usually occurred over near-circular failure planes.

2. Method

In the scope of this study, Şırnak asphaltite quarries 1 and 2 in the 940–830 m elevations and 920–810 m elevations. The slope stability analysis for the critical shale slopes were made. The shear stress change corresponding to the creep parameters of rock masses were concluded with tests *in situ* wire extensometers placed. In addition, the RQD and RMR values calculated on the logs as illustrated in **Figure 5** are compared with the values obtained as a result of the freeze-thaw analysis. Later GEO5 stability analysis is carried out to provide operational safety in the quarries in the mine management.

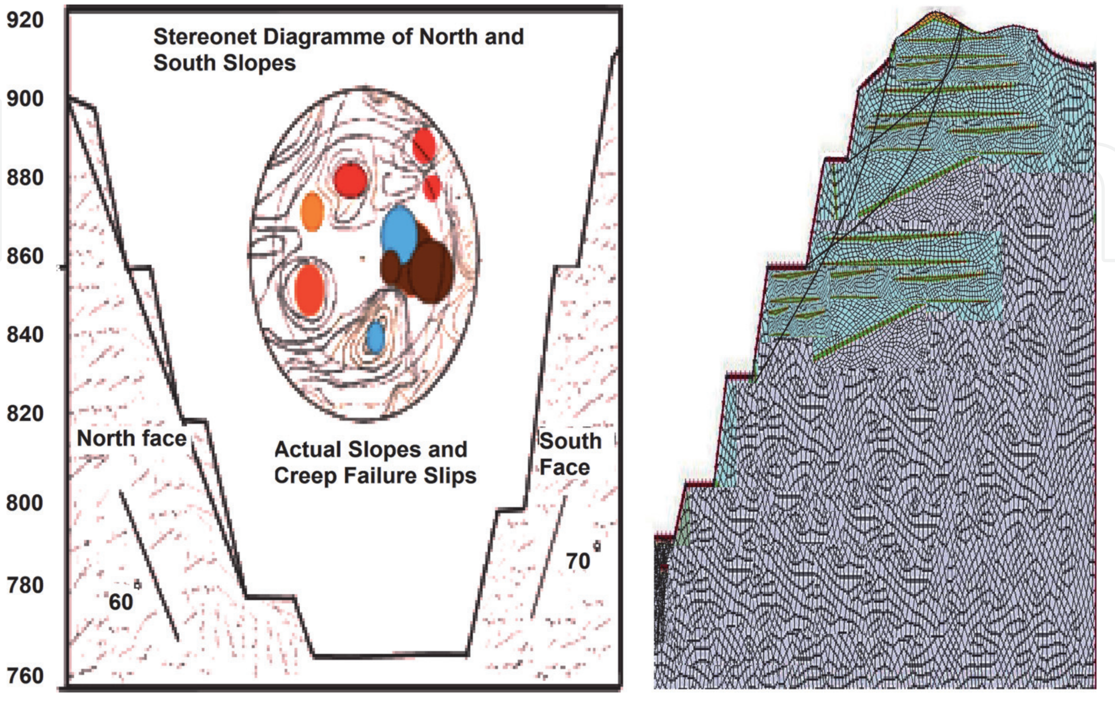

Figure 2.
North and south steep slope face of Avgamasya No 1 pit of Şırnak asphaltite coal mine site and sliding surfaces on a steep slope in the survey area.

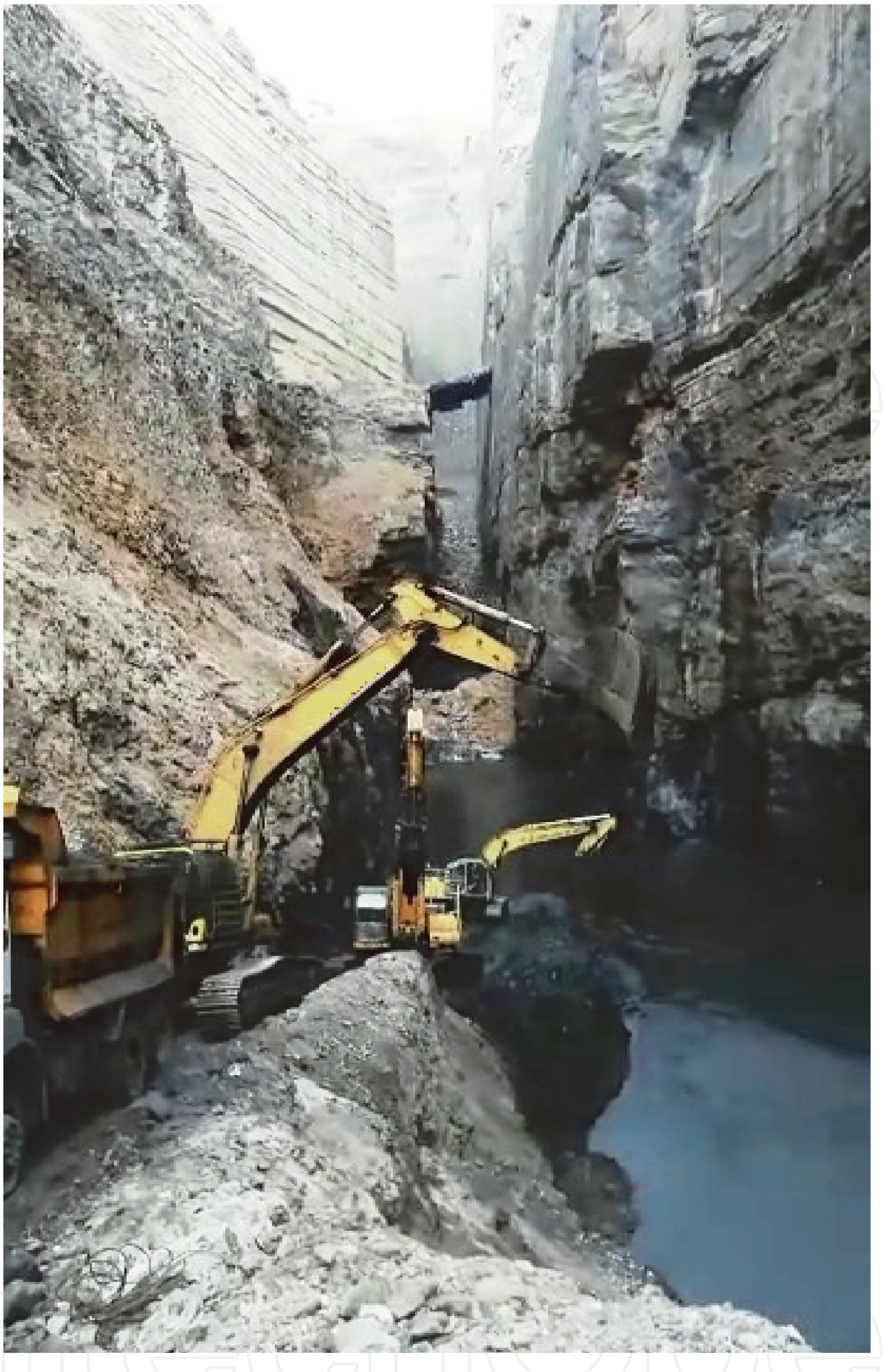

Figure 3.
North and south steep slope faces of Avgamasya No 1 and 2 pit survey area.

2.1 Rock mass properties in asphaltite quarry in Şırnak

2.1.1 RMR and RQD

Determination of rock mass properties by RMR method as a result of field studies, RMR and RQD crack counting for shale Jurassic alluvial unit of Pliocene aged are carried out to provide rational stability analysis on creep base regarding two months saturation time cycle. The study area has a lot of facing cracks and cores suitable for determining RQD from the field. RQD value measured as a result of discontinuity in a meter scale line as standard studies is given in **Figure 5**.

RMR score was determined for the determined RQD value and scoring is shown in **Figure 4**. Uniaxial compressive strength UCS and RMR scores of discontinuity

Figure 4.
South steep slope faces of Avgamasya No 1 pit of survey area.

Figure 5.
Shale and alluvium logs of south steep slope faces of Avgamasya No 1 pit survey area.

gap measurements (**Figure 5**) and RMR value and rock classification are presented in **Tables 2** and **3**.

RQD value as scoring for two soft limestones of early Eosins' and Miocene aged in Avgamasya were determined as 45 and 40 scores, respectively. It is concluded that the limestone unit is of medium rock quality and the shale and alluvial unit Pliocene aged is of poor rock quality.

2.2 Pore pressure

The geological rock classification method is useful for slope stability analysis even for complex rock and soil formations. There was a real issue for alluvial pore

Rock formations	Thickness (m)	RQD (%)	c′ (kPa)	φ′	P1 (MPa)	I1 (MPa) (50 mm)	Shear strength (mm/s)	γsat n (g/cm$^{3)}$)	γdry (g/cm$^{3)}$)
S1	25	20.9	700	17	12.0	0.6	34	2.62	**2.48**
S2	34	22.9	1300	22	15.0	1.1	33	2.65	**2.47**
S3	35	30.8	1300	23	26.0	1.5	24	2.67	**2.52**
S4	27	35.9	2700	28	48.0	2.2	14	2.69	**2.51**

Table 2.
Results from geotechnical tests on samples taken from landslide slopes.

Rock no	S1	S2	S3	S4
γsat max (g/cm^3)	2.92	2.85	2.87	**2.67**
w_{opt} (%)	15.9	11.9	11.0	**12.3**
Permeability (k) (cm/s)	5.3×10^{-4}	3.0×10^{-5}	6×10^{-5}	$\mathbf{5.3 \times 10^{-4}}$

Table 3.
Proctor of ground samples and permeability test results.

pressure and rock pore pressure difference and even crack propagation changes the pore pressure in the rock layer put in the calculation. The alluvial soft rock properties are given in **Table 3**.

The pore pressure changing the strength of limestone is illustrated in **Figure 6**.

2.3 UCS compression strength

Samples with volumes 0, 1, 3, and 5% are soaked in water-filled jar. The advantage of this experiment is that it minimizes the errors of the course over 50 mm according to the standard freeze-thaw propagation [15–20]. The UCS change with pore content changing the two limestones, alluvium, and shale in the quarry is illustrated in **Figure 7**.

Considering inferences, extreme deformations can be observed undersaturated with water of pores depending on time. Due to these negative weight effects, various stress changes on complex texture are required for the stable sliding surface in order to reduce cracking and prevent the negative consequences of permeability on the slippery creep. Lower porosities and cracks are seen in two soft limestones. The alluvium and shale reached 22 and 45% cavities by cracking effects of creep.

The pore content of the shale sample containing 30% saturation was determined as 30.5% strength reduction and the maximum dry unit volume weight was 2.85 kN/m^3. Altered limestone reaches a pore saturation of 25% and the maximum dry unit weight of 2.6 kN/m^3 for Şırnak asphaltite quarry (**Figure 8**).

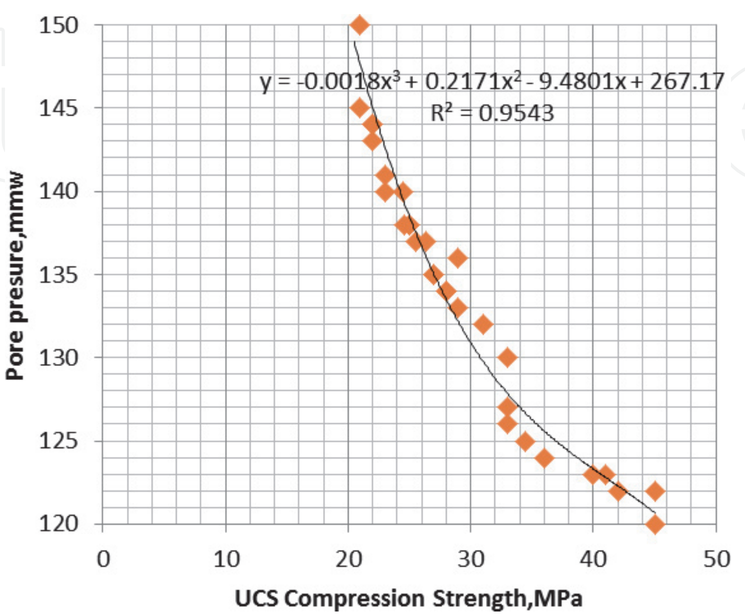

Figure 6.
The UCS compression strength change by pore pressure of soft limestone in Avgamasya asphaltite quarries No 1 and 2.

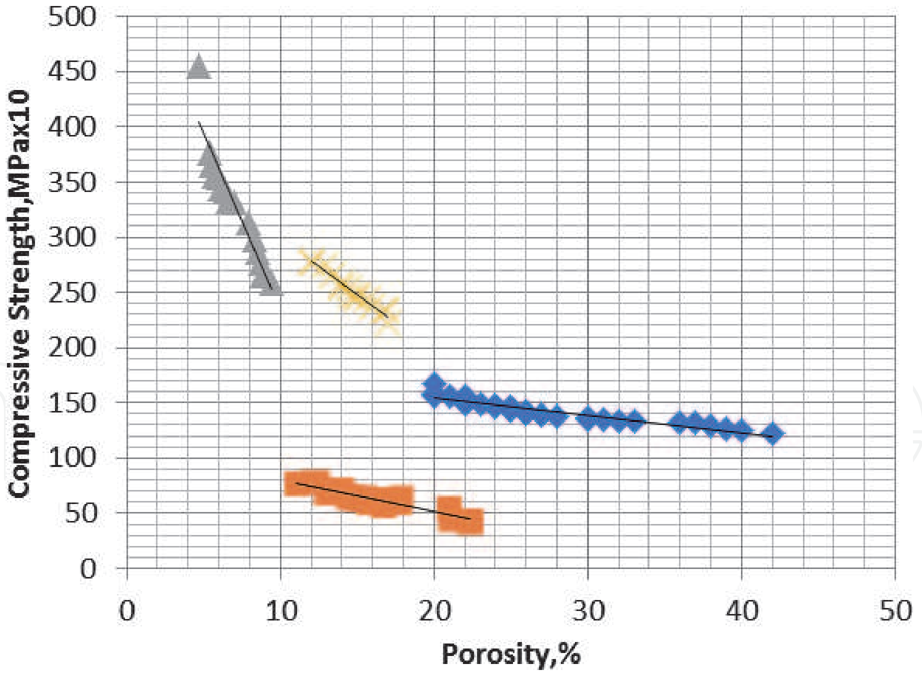

Figure 7.
The UCS compression strength of soft limestones, alluvium, and shale in Avgamasya quarry No 1/2.

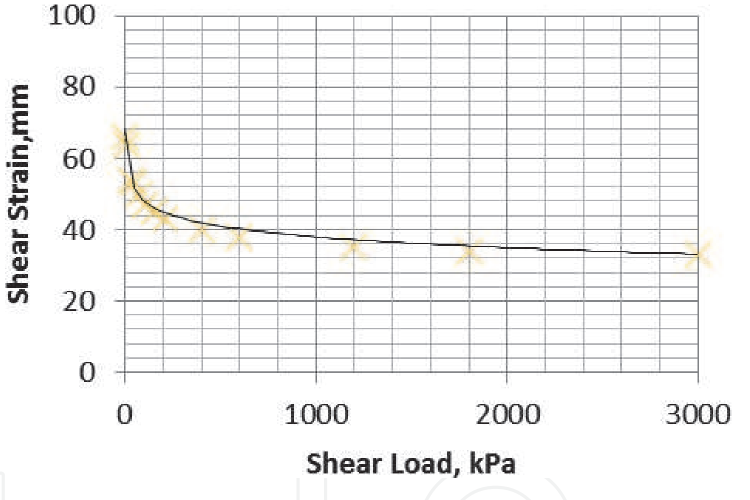

Figure 8.
The shear strain change for Şırnak shale at saturated pore pressure without any creep time for soft limestone.

2.4 Shear strength

The sawing indentation depth for soft and porous rock stones changed by rock microstructure and pore size as given below Eqs. (1) and (2); [16, 17].

Considering filling material by creep moves, extreme deformations can be observed under saturated sliding surfaces depending on time till 35–40 mm scale relative control length at 10 m wire. Due to slippery filling shale mud fines affected uncohesive free slippery surfaces, even internal change on internal friction angle loses caused for the instable sliding surface with increase cracking and prevent the negative consequences of instability on the slippery creep surface.

$$Deformation(cr) = -af \sum_{m=1}^{M} Lcr(1+r)^{m} \tag{1}$$

$$E\ Elasticity(cr) = f\sum_{m=1}^{M} Lcr(1+r)^{m} \tag{2}$$

After this shear process at 70 mm cylindrical disks, the strain amount of the box was determined from the electronic measuring stick on the device. Some samples taken from the submerged part of the box were dried in the oven and the water content corresponding to the pore saturation at the end of the test was found (**Figure 9**).

3. Creep failures of rocks

The stability is provided by water discharge resulted in low deformations of 10–20 mm can be observed under low water pressures of 10 mmw depending on time. The higher weight load of slope slices increases resistive stress change on complex sliding surface texture for the stability with reduction cracking and prevents the negative consequences of permeability on the slippery creep. Eq. (3) shows shear stress with deformation amount θ at time t [30]:

$$\mathrm{u}(\mathrm{x};\mathrm{t};\theta) = \sum_{i=0}^{n} \mathrm{u}(\mathrm{x},\mathrm{t}) + \phi(\mathrm{x};\mathrm{t};\theta).e^{-ti\theta} \tag{3}$$

4. Results and discussions

4.1 GEO5 slope stability analysis on creep theory

GEO5 model weight slice chart construction carried out as given below serial Eqs. (4)–(7) sum [36–41]:

$$F = \sum_{0}^{\mathrm{i}} \mathrm{N}_i\mathrm{F}_\mathrm{i} = \mathrm{N}_i\frac{C_\mathrm{i}}{\gamma H}\cos\beta^{i} \tag{4}$$

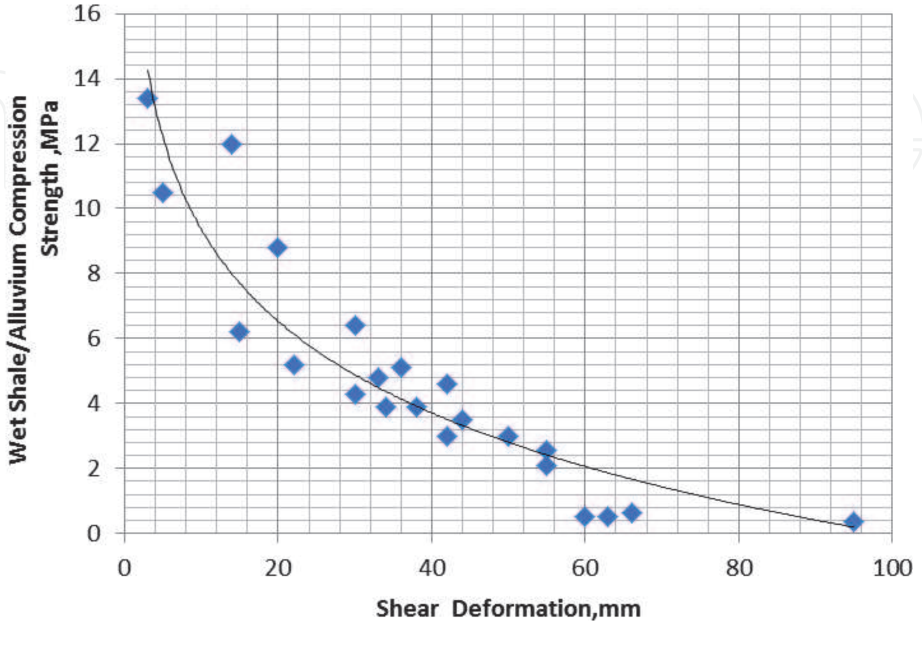

Figure 9.
The shear strength changes by sawing indentation regarding hardness factor of rock depending on creep porosity change by the time.

N_i slice weights the load F_i kN, anisotropic cohesion value of $\frac{C_1}{C_i}$, β free creep slope angle. The free slip surface stability weights show resistance by load chart slice calculations depending on slip surface angle and creep effect. Safety scorings calculated by this resistance to shear should be over 1.35 confirming the stability.

Regarding the crack orientation and intersection with water pore pressures changed by creep (**Figure 6**) in Eq. (5) shear factor R_c varied by slip surface angle exponential rate.

About 2–3 m length slice at i discontinuity at the angle of crack and creep propagated crack density and percentage distribution on slip surface change of $\frac{dy}{dx}$ was calculated by integral as given below Equations 5, 6.

$$R_c = \sum_0^i R_i F_i \tan\theta = \int_a^b e^{-ti\theta} dy^i \tag{5}$$

$$\frac{dy}{dx} = e^{-ti\theta} dy \tag{6}$$

The studied areas shear loads were regressed as exponential functions given below:

The stability mechanism and control by creep crack propagation and creep pore pressure effect for each slice as given in Eq. (7)

$$\frac{dy}{dx} = u = \sum_0^i R_i F_i / \tan a \left(1 - e^{-tRi/\mu}\right)^i \tag{7}$$

u shear deformation by highlighted in the creep theory, the lowered intrinsic friction resistance, F weight slice, a shear fracture inclination angle t time, μ crack free low viscosity at i weight slice.

The safety scoring in toppling and creep flow or landslide is calculated by following the shear force and resisting load over the slope as shear deformations based on the lowered internal friction angle patterns. Rock falling caused by cohesion-free bottom cracking and propagated shear dislocations and pore pressures can be observed in free-fall displacements above 40 mm displacements. The stability analysis carried out by calculations depending on the crack propagation overslip surface for each slice was calculated by the Eqs. (8)–(15) sequentially as below:

$$Ji = \sum_0^i N_i F_i \tan a_i \tag{8}$$

$$Ri = \sum_0^i S_i W_i \cos a_i = \tag{9}$$

$$p_u = \frac{\Upsilon'}{\Upsilon} H_i \tag{10}$$

$$Fi_u = \sum_0^i W_i \sin a_i - S_u = \sum_0^i W_i - p_u \tag{11}$$

$$S_{iu} = \sum_0^i c_u' l \; sec\, a_i + Fi_u \frac{\Upsilon'}{\Upsilon} H_i \tan^2\phi' \leq 1.25 \tag{12}$$

$$\sigma'_{\theta} = \sigma - u_a + \chi(u_a - u_{wi}) \tag{13}$$

$$\tau_{\theta i} = c'_i + (\sigma - u_a + \chi(u_a - u_{wi}))\ \tan\phi' \tag{14}$$

$$\mathrm{S_{iu}} = \sum_{0}^{i} \mathrm{c}_u{}'l\ sec\, a_i + (\sigma - u_a + \chi(u_a - u_{wi}))\ \tan^2\phi' \leq 1.25 \tag{15}$$

The safety scoring of S_{iu} water-saturated effective mechanical strength parameters regarding creep failure.

5. Slope analysis of S1, S2 and S3 shale soil/rock face slopes

The top alluvium shale heterogeneous benches of S1, S2, and S3 benches following closed excavation period of winter December and January term started deformation shears at 10 mm sized and the cracks propagated at 11% more and 2 mm widened size gaps caused the little movements that observed and measured in field studies. In quarry No 2, S3 showed free developed slip with top alluvium bench covered with alluvium 10 m sliding depth at steep bench rock stability analyzed by GEO5 programs. The results showed a slip failure problem due to heterogeneous structure and complexity with the wet saturated sliding surface over high 40% saturation on slip surface as given in **Table 4** (**Figures** 7 and **10**). In quarry No 1, top shale bench S2 showed similar lowered stability as given in **Table 5** and shown in **Figure 11**. The top bench of soft limestone at slice showed better stability safety factor as given in **Table 6** and illustrated in **Figure 11** as the higher stack and even the maximum height difference between the heel points 30–35 m, the slope of the maximum height of 50 m, the slope of the surface tilt angle is 60°.

The calculation style given in **Tables 4-6** are the results of original wet and creep cohesive resistive parameters obtained from the soft shattered rock formations made in alluvium c′ = 0.9 kPa, φ′ = 20°, $\gamma_{sat.}$ = 2.57 g/cm^3 c′ = 0.4 kPa, φ′ = 21°, $\gamma_{sat.}$ =

Chart	Block height	Block width	Block weight ton	Block weight (kN)	Block shear (MPa)	Resistance to shear (MPa)	Safety	Creep
1	3	4	1.33	13.09	0.77	0.66	1.53	1.32
2	5	6	3.34	32.73	1.62	1.35	1.29	1.08
3	10	8	8.90	87.27	3.97	3.26	1.19	0.98
4	15	9	15.01	147.27	6.57	5.37	1.16	0.95
5	18	7	14.01	137.45	6.14	5.02	1.17	0.95
6	16	5	8.90	87.27	3.97	3.26	1.19	0.98
7	14	4	6.23	61.09	2.84	2.34	1.21	1.00
8	11	4	4.89	48.00	2.28	1.88	1.24	1.03
9	9	3	3.00	29.45	1.47	1.23	1.31	1.09
10	7	3	2.34	22.91	1.19	1.00	1.36	1.14
Total			7.55	666.52	30.82	25.38	1.21	0.99

Table 4.
Weight chart calculations for S1 creep sliding on alluvium.

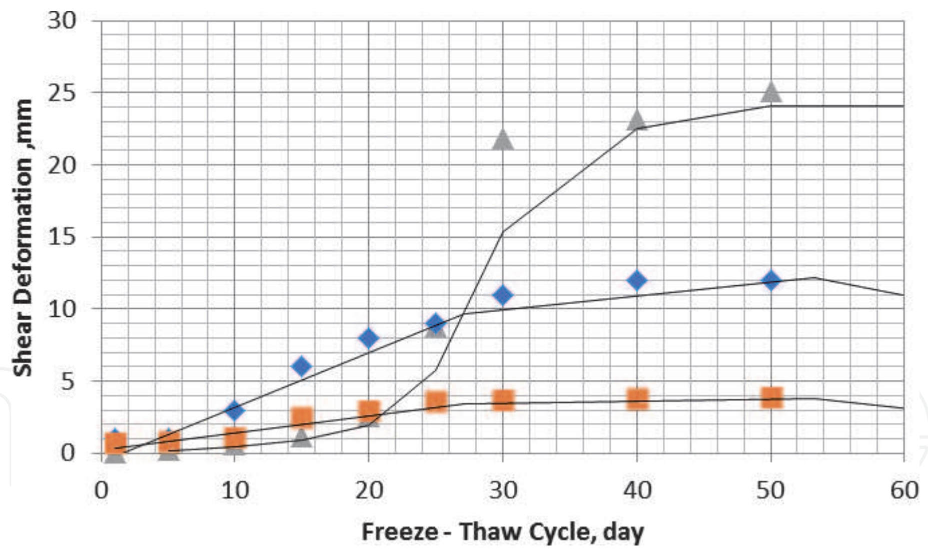

Figure 10.
Creep deformation by time over freeze-thaw time cycle as day periods for soft limestone, alluvium, and shale.

Chart	Block height	Block width	Block weight (ton)	Block weight (kN)	Block chart share (MPa)	Resistance to shear (MPa)	Safety	Creep
1	1.7	2.0	3.34	32.73	1.90	1.62	1.52	1.29
2	2.3	2.3	5.45	53.45	2.97	2.51	1.45	1.23
3	4.0	2.7	10.68	104.72	5.64	4.73	1.41	1.18
4	5.7	3.0	17.01	166.90	8.86	7.42	1.39	1.16
5	6.0	2.3	14.01	137.45	7.33	6.14	1.39	1.17
6	5.7	1.7	9.45	92.72	5.01	4.21	1.41	1.19
7	5.0	1.3	6.67	65.45	3.60	3.03	1.44	1.21
8	4.0	1.3	5.34	52.36	2.92	2.46	1.46	1.23
9	3.0	1.0	3.00	29.45	1.73	1.47	1.53	1.31
10	2.3	1.0	2.34	22.91	1.39	1.19	1.58	1.36
Total			8.59	758.16	41.35	34.79	**1.42**	**1.20**

Table 5.
Weight chart calculations for S2 creep sliding on soft limestone.

2.57 g/cm^3 in shale, and c′ = 1.7 kPa, φ′ = 25°, $\gamma_{sat.}$ = 2.62 g/cm^3 in soft limestone are used to score safety value. According to calculated safety scores on the potential free creep, surface deformation is lowered to 32° slope as seen in **Figure 11**.

The fracture or discontinuity angle t frequency% in the 20 m sliding on slope direction and the variable position in the design card $\frac{dy}{dx}$ were calculated as give below equations and **Tables 4-6**.

$$R_c = \sum_{0}^{i} R_i F_i \tan\theta = \int_a^b e^{-ti\theta} dy^i \tag{16}$$

$$\frac{dy}{dx} = e^{-ti\theta} dy \tag{17}$$

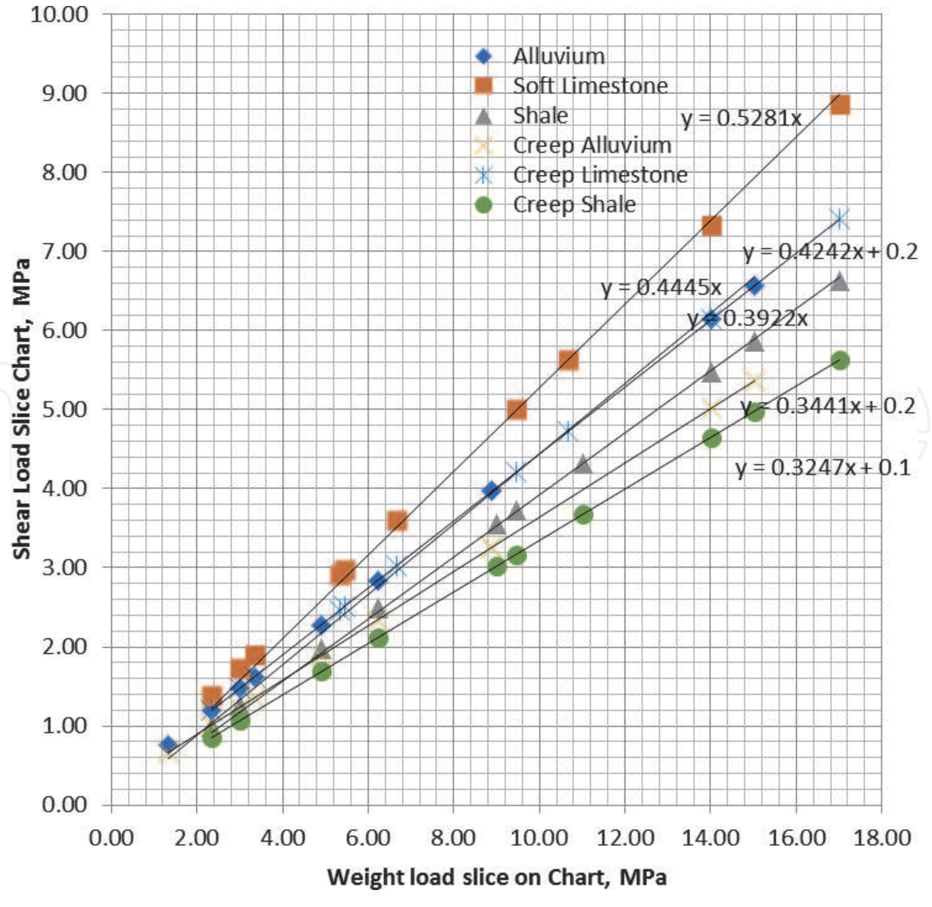

Figure 11.
The shear resistivity on slice weight chart calculations and GEO5 stability analysis for soft limestone, alluvium, and shale with creep.

Chart	Block height	Block width	Block weight (ton)	Block weight (kN)	Block shear (MPa)	Resistance to shear (MPa)	Safety	Creep
1	3.0	3.0	9.01	88.36	3.56	3.03	1.05	0.89
2	3.7	3.0	11.01	108.00	4.32	3.68	1.05	0.89
3	5.0	3.0	15.01	147.27	5.86	4.98	1.04	0.88
4	5.7	3.0	17.01	166.90	6.63	5.63	1.04	0.88
5	6.0	2.3	14.01	137.45	5.48	4.65	1.04	0.88
6	5.7	1.7	9.45	92.72	3.73	3.17	1.05	0.89
7	4.7	1.3	6.23	61.09	2.49	2.12	1.06	0.91
8	3.7	1.3	4.89	48.00	1.98	1.69	1.08	0.92
9	3.0	1.0	3.00	29.45	1.25	1.08	1.11	0.95
10	2.3	1.0	2.34	22.91	1.00	0.86	1.14	0.98
Total			10.22	902.15	36.28	30.86	1.05	0.89

Table 6.
Weight chart calculations for S3 creep sliding on shale.

The safety risk parameter was calculated as 1.42 stable for 40° slopes, but 50° and 60° slopes the safety factors decreased to 1198 and 1060. As given in figure the equation slope 44.2° has given the safety factor for a stable slope as 1120 is shown in **Figure 11**.

$$S = \frac{\sum(c' + \sigma' \cdot \tan\phi') \cdot \ell}{\sum(W \cdot \sin\alpha)} \tag{18}$$

Data obtained as a result of GEO5 steep discontinuity line studies regarded by shale and alluvial contact layers. The lower internal friction angle and cohesion was giving the safety factor of safety below 1.35 due to a sharp 15–25 m long sliding surface.

In this study, in the estimation of rock mass strength, RQD value for shale and alluvial zone as a result of RQD as an alternative to the method specified forward 41 and 35, respectively (**Table 1**). Use the normal stress(s) value when determining the strengths; m value to be used in GEO5 circle sliding surface analysis on creep base with defeat criterion from 3 for shale, 2 for alluvial clay, and a 35° slope are calculated as a function of RMR shale unit its value be 30 RMR crack propagation as determined at the end of creep period for limestone and shale alluvium.

In laboratory experiments for soft limestone rock, uniaxial test strength 42 MPa, dry unit weight 25.8 kN/m^3, shale uniaxial compressive strength of the rock 12 MPa, dry unit volume and its weight was determined as 24.45 kN/m^3.

2-4 month periods in the winter term results in severe weathering. RQD score is determined as the sum of the cracks and cracks filling points.

6. Conclusions

In this study, two different slope instabilities occurring in the enterprise were investigated. Extremely fractured, fractured, and altered creep saturated units were loaded to software as fill material as sliding saturated creep evaluated by the GEO5 slice analysis method.

The rock mass creep was based on the shear. It was demonstrated using the Hoek–Brown failure criterion. GEO5 FEM analysis was not chosen for the heterogeneous sliding manner. The shear stress-normal stress graphs gave higher safety values for long sliding surfaces. The slice charts as seen from **Figure 11**, the Avgamasya slopes 1, 2, 3, and 4 in the quarries 1 and 2 for two-dimensional (2D) and three-dimensional (3D) evaluation carried out. The hazard of the sharp slopes in the deep quarry was controlled with the slope stability analyses. The safety coefficients over 1.35 should be considered for steep bench slopes and improved safety working area in bench slopes prepared in Avgamasya asphaltite mining operations. There is also a great creep issue in slope stability is one of the biggest problems. The high pore water saturation comes out of hazardous free sliding. Before instability results arise on slopes various precautions and reinforcement methods or appropriate slope design preventing creep failures by applying top alluvial layer geometry, lower slope angels will be necessary for the security of production. For this reason, the displacement on the slopes that are likely to be defeated your angels regularly followed up with monitoring systems.

Finally, the high rainwater conditions or hard and long winter conditions are forced to creep analysis with slope stability charts practiced over the study area.

The 10–40 m long slip surfaces may cause free landslides unexpected in the quarry. The possibility of creep failure land flows may cause fatal accidents for asphaltite coal excavation areas. The stability analysis calculation should be carried out over highly shattered representative specimens at wet saturated effective strengths geotechnical parameters and the results should consider free land flows and tumbling rockslide prevention. The precautious methods appropriate for the asphaltite quarry were water discharge on the site to prevent instability within the scope of the creep in the quarries in the region.

Freeze-thaw cycling in 60 days or two months period decreased the strength values by about 34% over a month period for shale and alluvium. The pore ratio was also similar in the limestone samples. It was increased saturation by 27%. The creep values were also obtained in the shear box strength test.

Creep conditions depending on the pore density in the development of cracks and consequently the formation of wet saturated surfaces and lower shear resistance were observed.

Water discharge over alluvium and shale infiltration of rainwater through the rock slope mass will slow down creep matter and reduce free landslide or flow.

Abbreviations

c'	effective cohesion (kg/cm^2)
c	cohesion (kg/cm^2)
Φ'o	effective internal friction angle
Φo	internal friction angle
τ	shear stress (kg/cm^2)
σ	normal stress (kg/cm^2)
Is	point load index
Bs	bending strength
Ps	compression strength
Wopt	optimum water content
$\gamma_{Natural}$	natural unit volume weight (g/cm^3)
$\gamma_{Saturated}$	saturated unit volume weight (g/cm^3)
γ_{Dry}	dry unit volume weight (g/cm^3)
γkmax	maximum dry unit volume weight (g/cm^3)
γs	grain unit volume weight (g/cm^3)
k	permeability coefficient
S1, S2, S3, S4, C1, C2	south and north landslide risk slopes no. 1, 2, 3, 4
S11, C11	sample taken from south and north landslide risk slopes no.

Author details

Yildirim İsmail Tosun
Engineering Faculty, Mining Engineering Department, Şırnak University, Şırnak, Turkey

*Address all correspondence to: yildirimismailtosun@gmail.com

References

[1] Highland LM. Landslide Types and Processes, U.S. Department of the Interior, U.S. Geological Survey, Fact Sheet 2004-3072. 2004. Available from: https://pubs.usgs.gov/fs/2004/3072/fs-2004-3072.html

[2] Highland LM, Bobrowsky P. The Landslide Handbook—A Guide to Understanding Landslides. Vol. 1325. Reston, Virginia: U.S. Geological Survey Circular; 2008. p. 129. Available from:. https://pubs.usgs.gov/circ/1325/

[3] Hang Lin, Wenwen Zhong, Wei Xiong, Wenyu Tang, 2014. "Slope Stability Analysis Using Limit Equilibrium Method in Nonlinear Criterion", The Scientific World Journal, Hindawi P., vol. 2014, Article ID 206062, 7 pages, https://doi.org/10.1155/2014/206062

[4] Kliche, C. A., 1999. Rock Slope Stability, Society for Mining Metallurgy, SME, Penslyvania, USA, ISBN-10 978 0873351711, 253 p

[5] Kliche, C. A., 2018. Rock Slope Stability, 2nd Edt, Society for Mining, Metallurgy, and Exploration (SME) Penslyvania,USA, ISBN 978-0-87335-369-4

[6] Bieniawski ZT. Engineering Rock Mass Classification. Vol. 1989. New York: Wiley–Interscience; 1989

[7] Bieniawski ZT. Mechanism of brittle failure of rock Part I—Theory of fracture process. International Journal of Rock Mechanics and Mining Sciences. 1967;**4**(4):395-406

[8] Anonymous, 2011. Şırnak Provincial Administration Reports. Şırnak Municipal Bureau, Şırnak, Turkey

[9] Anonymous. Turkey Earthquake Zone Map. Disaster and Emergency Management Bureau, Earthquake Department Ankara; 2011

[10] Anonymous, 2013, GEO5 programs - Engineering Manuals—Part 1–Part 2 http://www.finesoftware.eu/geotechnical-software/, Zaverka Chechk Republik

[11] Anonymous. 2009. GEO5 programs. FEM. Theoretical Guide. Available from: http://www.finesoftware.eu/geotechnical-software/

[12] Tosun Yİ. Asphalt fill strengthening of free slip surfaces of shale slopes in asphaltite open quarry: Stability analysis of free sliding surface for wet shale slopes in Avgamasya Asphaltite Open Quarry No 2. Site, Chapter 5. In: Kanlı AI, editor. Slope Engineering. Rijeka: InTech; 2021. pp. 141-170. DOI:10.5772/intechopen.94893. ISBN: 978-1-83962-924-2, Print ISBN: 978-1-83962-923-5, eBook (PDF) ISBN: 978-1-83962-946-4

[13] Tosun Yİ. Anchorage pile strengthening of shale slopes and cementing falling stone blocks by mixture of melted waste plastics/asphalt and fly ash for slope stability in asphaltite open pit mining site in Avgamasya, Şırnak, Chapter 8. In: Soni A, editor. Mining Techniques—Past, Present and Future. Rejika: InTech; 2021. pp. 141-170. p. 208. DOI: 10.5772/intechopen.69927. ISBN 978-1-83962-369-1

[14] Tosun Yİ. Şırnak ve Cizre Yörel Yerleşim Alanlarındaki Heyelanların Jeoteknik Analizi, Olası Heyelan Tehlike Değerlendirmesi ve Haritalaması, Chapter 3. In: Kiliç GB, Çifçi ÜA, Yilmaz ÜA, editors. Mühendislik Alanında Araştırma ve Değerlendirmeler. Ankara: Gece Kitaplığı, Çankaya; 2019. pp. 35-50. ISBN: 978-605-7631-33-6

[15] ASTM C666/C666M-15. Standard Test Method for Resistance of Concrete

to Rapid Freezing and Thawing. West Conshohocken, PA: ASTM International; 2015. Available from: www.astm.org

[16] ASTM D3080/D3080M-11. Standard Test Method for Direct Shear Test of Soils Under Consolidated Drained Conditions (Withdrawn 2020). West Conshohocken, PA: ASTM International; 2011. Available from: www.astm.org

[17] ASTM D7012-14. Standard Test Methods for Compressive Strength and Elastic Moduli of Intact Rock Core Specimens under Varying States of Stress and Temperatures. West Conshohocken, PA: ASTM International; 2014. Available from: www.astm.org

[18] ASTM D6024/D6024M-16. Standard Test Method for Ball Drop on Controlled Low Strength Material (CLSM) to Determine Suitability for Load Application. West Conshohocken, PA: ASTM International; 2016

[19] ASTM D6067/D6067M-17. Standard Practice for Using the Electronic Piezocone Penetrometer Tests for Environmental Site Characterization and Estimation of Hydraulic Conductivity. West Conshohocken, PA: ASTM International; 2017

[20] ASTM D5878-19. Standard Guides for Using Rock-Mass Classification Systems for Engineering Purposes. West Conshohocken, PA: ASTM International; 2019

[21] Gorzelanczyk T, Schabowicz K. Effect of freeze–thaw cycling on the failure of fibre-cement boards, assessed using acoustic emission method and artificial neural network. Materials (Basel). 2019;**12**(13):2181. DOI: 10.3390/ma12132181

[22] Hoek E, Bray JW. Rock Slope Engineering. Hertford: Stephen Austin and Sons, Ltd; 1977. p. 402

[23] Lamp WT, Whitman RV. Soil Mechanics. New York: John Wiley and Sons; 1969

[24] Bishop AW. The use of the slip circle in the stability analysis of earth slopes. Geotechnique. 1955;**5**:7-17

[25] Hoek E. Estimating the stability of excavated slopes in Opencast mines. Institution of Mining and Metallurgy. 1970;**A105**:A132

[26] Paşamehmetoğlu LV, Özgenoğlu A, Watermelon C. Rock Slope Stability. 2nd ed. T.M.M.O.B Mining Eng: Bureaou Publications, Ankara; 1991

[27] Anbalagan R. Landslide hazard evaluation and zonation mapping in mountainous terrain. Engineering Geology. 1992;**32**:269-277

[28] Görög P, Török A. Slope stability assessment of weathered clay by using field data and computer modeling: a case study from Budapest. Natural Hazards and Earth System Sciences. 2007;**7**:417-422. Available from: www.natu-hazards-earth-syst-sci.net

[29] Görög P. Stability Problems of Abandoned Clay Pits in Budapest, IAEG 2006, Paper Number 295. The Geological Society of London; 2006

[30] Dramis F, Sorriso-Valvo M. Deep-seated gravitational slope deformations, related landslides and tectonics. Engineering Geology. 1994;**38**:231-243

[31] Hoek E. Practical Rock Engineering, notes by Evert Hoek Hoek. 2013. Available from: http://www.rocscience.co

[32] Hutchinson JN. Landslide hazard assessment. Keynote paper. In: Bell DH, editor. Landslides, Proceedings of 6th International Symposium on landslides, Christchurch, New Zealand. Vol. 1. Rotterdam: Balkema; 1995. pp. 1805-1841

[33] Prusa J. In: Vanicek et al., editors. Comparison of geotechnic softwares - Geo FEM, Plaxis, Z-Soil, XIII to ECSMG. Vol. 2. Prague. ISBN 80-86769-01-1: cgts; 2009

[34] Vaneckov V, Laura J, J Prus, 2011. Sheeting Wall Analysis by the Method of Dependent Pressures, Geotec Hanoi Geotec Hanoi 2011 "Geotechnics for sustainable development:"- ISBN 978-604-82-000-8 ID No. / pp. 7 Vietnam

[35] Venkatramaiah, C., 1993. "Stability of Earth Slopes" "Geotechnical Engineering", New Age Int. Pub., Trubati, India

[36] Tosun Yİ, Cevizci H, Ceylan H. Landfill Design for Reclamation of Şırnak Coal Mine Dumps—Shalefill Stability and Risk Assessment, ICMEMT 2014, 11-12 July 2014. Chekoslovakia: Prag; 2014

[37] Tosun Yİ. A case study on use of foam concrete landfill on landslide hazardous area in Şırnak City Province. In: XX Congress of the Carpathian Balkan Geological Association; 24–26 September 2014; Tirana, Albania. 2014

[38] Tosun Yİ. Shale stone and fly ash landfill use in land-slide hazardous area in Sirnak City with Foam Concrete. GM Geomaterials Journal. 2014;**4**(4): 141-150. DOI: 10.4236/gm.2014.44014

[39] Yıldırım İ. Tosun, 2016, Kalker, Marn ve Şeylin Sünme Karakterizasyonu - Bitümlü Gözenekli Agrega için Don—Mikrodalga Kurutma-Bilya Darbe Dayanım Testi ile Sünme Etüdü, AGGRE 2016, 8th Internatıonal Aggregates **Sy**mposıum; October 5–7; Istanbul, Turkey

[40] Tosun, Y.İ., 2016. Use of Modified Freeze-Drop Ball Test for Investigation the Crack Propagation Rate in Coal Mining- Case Study for the Şırnak Asphaltite Shale, Marly Shale and Marl in Şırnak Coal Site, IBSMTS 2016, 1th Internatıonal Black Sea Symposium on Mininig and Tunnelling, November 02–04; Trabzon, Turkey

[41] Török, Á. Bögöly, G., Czinder, B., Görög, P., Kleb, B., Vásárhelyi, B., Lovas, T., Barsi, Á., Molnár, B., Koppányi Z., and Somogyi, J. Á., 2016. Terrestrial laser scanner aided survey and stability analyses of rhyolite tuff cliff faces with potential rock-fall hazards, an example from Hungary, Eurock, Cappadicia, 877–881.

[42] Á Török, Á Barsi, G Bögöly, T Lovas, Á Somogyi, and P Görög, 2017. Slope stability and rock fall hazard assessment of volcanic tuffs using RPAS and TLS with 2D FEM slope modelling, Nat. Hazards Earth Syst. Sci. Discuss., Nat. Hazards Earth Syst. Sci., 18, pp. 583–597, doi:10.5194/nhess-2017-56, 2017

[43] Barton N, Lien R, Lunde J. Engineering classification of rock masses for the design of tunnel support. Rock Mechanics. 1974;**6**(4):189-236

[44] Bieniawski ZT. Engineering Rock Mass Classifications: A Complete Manual for Engineers and Geologists in Mining, Civil, and Petroleum Engineering. Hoboken, New Jersey: John Wiley & Sons; 1989

[45] Cai M, Kaiser PK, Tasaka Y, Minami M. Determination of residual strength parameters of jointed rock masses using the GSI system. International Journal of Rock Mechanics and Mining Sciences. 2007;**44**(2): 247-265

[46] Dong-ping D, Liang L, Jian-feng W, Lian-heng Z. Limit equilibrium method for rock slope stability analysis by using the Generalized Hoek–Brown criterion. International Journal of Rock Mechanics and Mining Sciences. 2016;**89**(June): 176-184

[47] Erguler ZA, Karakuş H, Ediz IG, Şensöğüt C. Assessment of design

parameters and the slope stability analysis of weak clay-bearing rock masses and associated spoil piles at Tunçbilek basin. Arabian Journal of Geosciences. 2020;**13**(1):1-11

[48] Hammah, R., Curran H, J., Yacoub, T., Corkum, B. 2004. Stability analysis of rock slopes using the finite element method. In Proceedings of the ISRM Regional Symposium EUROCK 2004 and the 53rd Geomechanics Colloquy, Salzburg, Austria

[49] Hoek E, Carranza C, Corkum B. Hoek-brown failure criterion. 2002 edition. Narms-Tac. 2002;**1**(1):267-273

[50] Hoek E, Kaiser PK, Bawden WF. Support of underground excavations in hard rock. Journal of Rock Mechanics and Mining Sciences. 2000;**35**(2):219-233

[51] Hoek E. Estimating Mohr-Coulomb friction and cohesion values from the Hoek-Brown failure criterion. International Journal of Rock Mechanics and Mining Sciences. 1990;**27**(3): 227-229

[52] Sheng H, Kaiwen X, Feng D. Establishment of a Dynamic Mohr–Coulomb Failure Criterion for Rocks. International Journal of Nonlinear Sciences and Numerical Simulation. 2012;**13**(2012):55-60

[53] Park J, Hyun C-U, Park H-D. Changes in microstructure and physical properties of rocks caused by artificial freeze–thaw action. Bulletin of Engineering Geology and the Environment. 2015;**74**(2):555-565

[54] Ning L, Jonathan G. Infinite slope stability under steady unsaturated seepage conditions. Water Resources Research. 2008;**44**:11404. DOI: 10.1029/2008WR006976

[55] Duncan JM, Wright SG. Soil Strength and Slope Stability. Hoboken, New Jersey: John Wiley; 2005. p. 297

[56] Hoboken NJ, Fredlund DG, Morgenstern NR, Widger RA. The shear strength of unsaturated soil. Canadian Geotechnical Journal. 1978;**15**:313-321

[57] Rahardjo HT, Ong H, Rezaur B, Leong EC. Factors controlling instability of homogeneous soil slopes under rainfall. Journal of Geotechnical & Geoenvironmental Engineering. 2007;**133**(12):1532-1543

[58] Bazant ZP et al. In: Bazant Z, editor. Chapter 3 Creep Analysis of Structures, Mathematical Modeling of Creep and Shrinkage of Concrete. Hoboken, New Jersey: John Wiley & Sons Ltd; 1988

[59] Hoek, E., Carranza, C., Corkum, B. 2002. Hoek-brown failure criterion – 2002 edition. 2002 Edition. Proceedings of the 5th North American Rock Mechanics Symposium, Toronto, 7-10 July 2002, 267-273.,Narms-Tac, **1**(1), 267–273.

[60] Wei Y, Jiaxin L, Zonghong L, Wei W, Xiaoyun S. A method based on the Generalized Hoek-Brown (GHB) criterion for strength reduction slope failure (Iran). Environmental Earth Sciences. 2020;**60**(1):183-192